Three-Dimensional Binocular Kinematics of Torsional Vestibular Nystagmus During Convergence on Head-Fixed Targets in Humans

O. BERGAMIN AND D. STRAUMANN
Department of Neurology, Zurich University Hospital, CH-8091 Zurich, Switzerland

Received 13 October 2000; accepted in final form 23 March 2001

Bergamin, O. and D. Straumann. Three-dimensional binocular kinematics of torsional vestibular nystagmus during convergence on head-fixed targets in humans. *J Neurophysiol* 86: 113–122, 2001. When a human subject is oscillated about the nasooccipital axis and fixes upon targets along the horizontal head-fixed meridian, angular eye velocity includes a vertical component that increases with the horizontal eccentricity of the line-of-sight. This vertical eye movement component is necessary to prevent retinal slip. We asked whether fixation on a near head-fixed target during the same torsional vestibular stimulation would lead to differences of vertical eye movements between the right and the left eye, as the directions of the two lines-of-sight are not parallel during convergence. Healthy human subjects ($n = 6$) were oscillated (0.3 Hz, ±30°) about the nasooccipital axis on a three-dimensional motor-driven turntable. Binocular movements were recorded using the dual search coil technique. A head-fixed laser dot was presented 1.4 m (far head-fixed target) or 0.25 m (near head-fixed target) in front of the right eye. We found highly significant ($P < 0.01$) correlations (R binocular = 0.8, monocular = 0.59) between the convergence angle and the difference of the vertical eye velocity between the two eyes. The slope of the fitted linear regression between the two parameters ($s = 0.45$) was close to the theoretical slope necessary to prevent vertical retinal slippage (predicted $s = 0.5$). Covering the left eye did not significantly change the slope ($s = 0.52$). In addition, there was a marked gain reduction (~35%) of the torsional vestibuloocular reflex (VOR) between viewing the far and the near targets, confirming earlier results by others. There was no difference in torsional gain reduction between the two eyes. Lenses of +3 dpt positioned in front of both eyes to decrease the amount of accommodation did not further change the gain of the torsional VOR. In conclusion, ocular convergence on a near head-fixed target during torsional vestibular stimulation leads to deviations in vertical angular velocity between the two eyes necessary to prevent vertical double vision. The vertical deviation velocity is mainly linked to the amount of convergence, since it also occurs during monocular viewing of the near head-fixed target. This suggests that convergence during vestibular stimulation automatically leads to an alignment of binocular rotation axes with the visual axes independent of retinal slip.

INTRODUCTION

During head movements, the vestibuloocular reflex (VOR) serves to stabilize the eyes in space. To keep the line-of-sight directed to a head-fixed target while the head rotates horizontally or vertically, the VOR must be cancelled; i.e., ideally, its gain becomes zero (Barnes et al. 1978; Zee 1977). If one extends the analysis to all degrees-of-freedom of eye rotations during vestibular stimulation (horizontal, vertical, and torsional), the description of the influence by visual fixation on the VOR cannot be restricted to the dynamic aspects (gain, phase) of the system, i.e., visual VOR-suppression, but must also consider the three-dimensional (3D) kinematics of eye rotation.

Misslisch et al. have shown that the angular velocity vector during visual VOR cancellation is oriented approximately parallel to the line-of-sight (Misslisch et al. 1996). This is a result of a 3D reorientation of the ocular rotation axes, such that retinal slippage is restricted to rotations about the line-of-sight. For instance, when subjects are oscillated about the nasooccipital axis in total darkness (=torsional VOR), the angular velocity axis tilts in the opposite direction to the gaze line by about half the angle (Misslisch et al. 1994). However, if the eyes fixate upon a head-fixed light dot, the angular velocity axis tilts toward the gaze line by roughly the full angle (Misslisch et al. 1996). Thus the angle between the ocular rotation axes during pure torsional VOR and during suppression of torsional VOR amounts one and a half times the gaze angle.

We asked whether these kinematical principles could also be applied to ocular movements during torsional VOR while the eyes converge on near head-fixed targets. Our hypothesis was that the binocular angular velocity vectors are no longer oriented in parallel, but align with the lines-of-sight. We predicted that the combination of convergence and torsional VOR results in a physiological "dissociation" of vertical eye movements when described in a head-fixed coordinate frame. In other words, the "correct" vertical deviation of movements between the two converging eyes during torsional VOR would produce "purely torsional" movements in eye-fixed coordinates to prevent double vision.

To test our hypothesis on convergence-induced reorientation of ocular rotation axes during vestibular roll stimulation, we measured the 3D movements of both eyes in healthy head-restrained human subjects during whole-body oscillation about the nasooccipital axis on a motorized turntable. During stimulation, subjects had to fix upon a head-fixed light dot at near or far distances.

METHODS

Subjects

Six healthy human subjects (2 female, 4 male; 32–55 y) gave consent and participated in this study after being informed of the experimental procedures. Protocols adhered to the Declaration of Helsinki for research involving human subjects (adopted by the 18th World Medical Assembly, Helsinki, Finland, 1964, and revised last in

Address reprint requests to D. Straumann (E-mail: dominik@neurol.unizh.ch).

The costs of publication of this article were defrayed in part by the payment of page charges. The article must therefore be hereby marked "*advertisement*" in accordance with 18 U.S.C. Section 1734 solely to indicate this fact.

Hong Kong in 1989), and were approved by the local Ethical committee.

Experimental setup

Subjects were tested on a turntable with three servo-controlled motor-driven axes (Acutronic, Jona, Switzerland). The head was restrained with an individually molded thermoplastic three-point-mask (Sinmed BV, Reeuwijk, The Netherlands). The subject's head was positioned such that the center of the interaural line was at the intersection of the three axes of the turntable. Evacuation pillows and safety belts minimized body movements. The head was surrounded by an aluminum coil frame (side length 0.5 m) by which three orthogonal magnetic fields with frequencies of 55.5, 83.3, and 41.6 kHz were produced. The synchronous detection of the amplitude-modulated signals yielded instantaneous voltages induced by the three magnetic fields (system built by A. Lasker, Baltimore, MD).

Eye movement recordings

Three-dimensional eye movements were recorded binocularly with dual scleral search coils (Skalar Instruments, Delft, The Netherlands) (Collewijn et al. 1985; Robinson 1963). For calibration, the voltage offsets of the system were zeroed by placing the search coils in the center of a metal tube to shield them from the magnetic fields. Then the relative gains of the three magnetic fields were determined with the search coils on a gimbal system placed in the center of the coil frame. Details of the calibration procedure can be found in detail elsewhere (Straumann et al. 1995).

After conjunctival and corneal local anesthesia with oxybuprocaine 0.4%, the search coil annuli were placed around the cornea of both eyes. Eye and chair movements were digitized at a frequency of 1,000 Hz with a 16-bit resolution and stored on a computer hard disk for off-line processing. The peak-to-peak noise levels of calibrated position signals were 0.2° in the torsional and 0.1° in the horizontal and vertical directions.

Experimental protocol

On the 3D turntable, subjects were seated in the upright position. The axis about which the turntable was oscillated during the subsequent paradigms coincided with the *x*-axis of the coil frame, i.e., the torsional or nasooccipital axis. During all paradigms, the turntable was sinusoidally rotated with a frequency of 0.3 Hz and an amplitude of ±30°. A head-fixed laser dot was projected onto screens 0.25 or 1.4 m in front of the right eye. The center of the right eye and these two targets formed a straight line that was parallel to the vestibular stimulation axis (Fig. 1). To make sure that the near target was exactly on the line through the center of the right eye parallel to the stimulation axis, the screen for the near target was transparent, and the subjects had to indicate on the screen the position that was precisely in front of the far target. This location was then marked with a circular non-transparent paper (3 mm diam), in the center of which a head-fixed laser was projected to serve as the near target.

Subjects were instructed to fixate and focus onto the far or near light dot such that it did not appear blurred. When both eyes converged on the far or near target, the line-of-sight of the left eye pointed $\phi_1 = 2.5°$ or $\phi_2 = 13.5°$ inward, respectively. An additional far laser dot (again at a distance of 1.4 m), positioned along the straight line between the center of the left eye and the near target, could be switched on.

Three paradigms (I–III) were used during torsional vestibular stimulation: I, fixation of the far target in front the right eye (left eye pointing to the right by the angle ϕ_1); II, fixation of the far target on the right (left eye pointing to the right by the angle ϕ_2); and III, fixation of the near target in front of the right eye (left eye pointing to the right by the angle ϕ_2 again). Each paradigm lasted 34 s.

Figure 1 schematically explains why we chose these target locations: the position of the right eye was the same in paradigms I and III, while the position of the left eye was the same in paradigms II and III. Hence the eye movements recorded during paradigms I and II served as control data for the eye movements recorded during paradigm III. In all three paradigms, subjects were tested during binocular fixation (I, II, and III) and during monocular fixation with the right viewing (I_R, II_R, and III_R). In addition, paradigm III was repeated with the subjects wearing glasses of +3 dpt in front of each eye (binocular: III^g; monocular: III^g_R). The reason for applying these lenses was to decrease the amount of accommodation associated with convergence. By adding the lenses we did not intend to completely cancel the need for accommodation in each subject individually, but to decrease accommodation in all subjects by a constant amount to study the kinematical effect of this optical intervention.

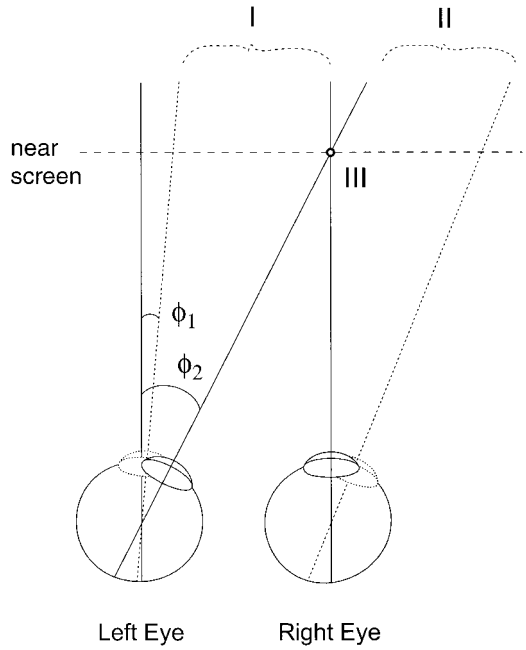

FIG. 1. Paradigms of binocular fixation of head-fixed targets during torsional vestibular stimulation. Angles are exaggerated (multiplied by a factor of 2) for clarity. I: fixation on far target (1.4 m) in front the right eye; II: fixation on far target (1.4 m) to the right; III: fixation on near target (0.25 m) in front of the right eye. ϕ_1: horizontal angle of the left eye during paradigm I. ϕ_2: horizontal angle of the left eye during paradigms II and III.

Data analysis

The data analysis was performed with an interactive program written with MATLAB Version 5.3. Three-dimensional eye positions were expressed as rotation vectors. A rotation vector $r = (r_x, r_y, r_z)$ describes the instantaneous orientation of a body as a single rotation from the reference position; the vector is oriented parallel to the axis of this rotation, and its length is defined by $\tan(\rho/2)$, where ρ is the rotation angle. The three head-fixed orthogonal axes of the coil frame defined the coordinate system of rotation vectors with the *x*-axis pointing forward, the *y*-axis leftward, and the *z*-axis upward. The signs of rotations about these cardinal axes were determined by the right-hand rule; i.e., clockwise, leftward, and downward rotations, as seen by the subject, were positive.

From the rotation vectors r, 3D velocity vectors ω were computed, using the formula (Hepp 1990)

$$\omega = 2(\mathrm{d}r + r \times \mathrm{d}r)/(1 + |r|^2)$$

where dr denotes the derivative of r and $\times$ the cross product. Angular eye-velocity vectors are oriented parallel to the instantaneous ocular rotation axis; their lengths are proportional to the velocity of rotation. For convenience, the lengths of rotation vectors and angular velocity

vectors were given in degrees (°) and degrees per second (°/s), respectively, but the right-hand rule was maintained when describing the orientation of these vectors.

Geometric considerations

Figure 2 depicts the rotation axes of the eyes during binocular fixation of far and near head-fixed targets during torsional vestibular stimulation in upright position. In this hypothetical scheme we assumed that the ocular motor system succeeds in stabilizing the head-fixed target point on the fovea in all three paradigms (I, II, and III).

Figure 2*A* shows the retina of both eyes from behind during ocular counterrolling in the clockwise direction (gray-shaded arrow). If the line-of-sight is parallel to the vestibular stimulation axis while fixating the far head-fixed target straight ahead, both eyes rotate about the line-of-sight, i.e., no additional vertical or horizontal movement is necessary for the stabilization of the head-fixed target point on the fovea (paradigm I). During binocular fixation of the far head-fixed target in right gaze, the same counterroll would move the fovea mainly upward (dotted arrow), unless there is a corrective downward movement component of the eyes. Without this vertical correction, the head-fixed target would slip vertically on the retina of both eyes (paradigm II). If a near head-fixed target is precisely in front of the right eye on a line that is parallel to the vestibular stimulation axis (paradigm III), the right eye must rotate as in paradigm I and the left eye as in paradigm II, in order to stabilize the head-fixed target on both eyes' fovea for binocular fixation.

Figure 2*B* illustrates the top view of the angular velocity vectors during the three paradigms. During binocular fixation of the far head-fixed target straight ahead, the angular velocity vectors of both eyes are aligned with the lines-of-sight and parallel to the vestibular stimulation axis (paradigm I). When the eyes fix upon the far head-fixed target to the right, both angular velocity vectors coincide again with the line-of-sights but deviate from the vestibular stimulation axis (paradigm II). Provided the gain (gain is eye velocity divided by turntable velocity) of counterroll is the same as in paradigm I, the torsional component of the angular velocity vectors remains the same, but an additional component has to be vectorially added for the appropriate vertical movement. If the subject fixes upon the near head-fixed target in front of the right eye and stabilizes the head-fixed

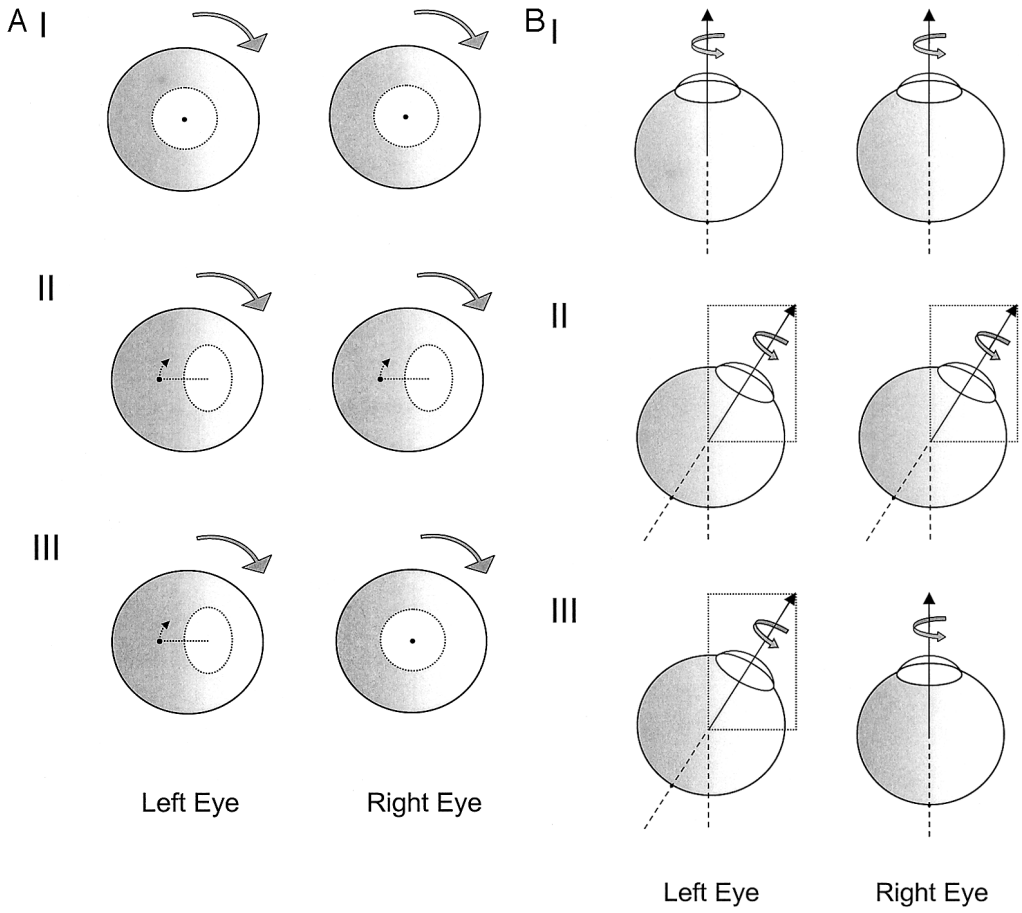

FIG. 2. Schematic head-fixed view of the two eyes seen (*A*) from behind and (*B*) from above during the 3 paradigms (I, II, and III) in the phase of ocular counterroll to the right (induced by head roll to the left). For better clarity, the small angle of the left eye during straight-ahead fixation onto the far target ($\phi_1 = 2.5°$) was omitted (= target located at infinite distance). The figure assumes that both eyes always rotate about their lines-of-sight. *A*: the gray arrow indicates the rotation of the ocular globe induced by the turntable oscillation (ocular counterroll). The corneal limbus is depicted by the dashed circle or ellipse. If the ocular rotation axes coincide with the line-of-sight, the retinae rotate such that the fovea is not displaced. If, on the other hand, the ocular rotation axes stayed parallel to the nasooccipital axis of vestibular stimulation, the fovea would move mainly upward (dotted curved arrow). *B*: the black solid arrows represent the angular velocity vectors, which align with the respective lines-of-sight. The gray arrows give the direction of rotation. I: when fixating the far head-fixed target straight ahead, both eyes rotate about axes parallel to the stimulus axes. II: when fixating the far head-fixed target to the right, ocular counterroll rotates both foveae in the upward direction (*A*), but not if the angular velocity vectors of both eyes are shifted to point towards the head-fixed target (*B*). Thus, by adding a vertical velocity component, the visual target is stabilized on both foveae. III: when fixating the near target in front of the right eye, ocular counterroll would move the left eye's fovea away from the target (*A*), but if a vertical velocity component is added such that the angular velocity vector points towards the target, the fovea of the left eye is also stabilized.

target on both eyes' fovea (paradigm III), the angular velocity vector of this eye must point straight ahead and be purely torsional (as in paradigm I), while the angular velocity vector of the left eye must point to the right (as in paradigm II). Note that the components of the angular velocity vectors (horizontal, vertical, torsional) are in a head-fixed coordinate frame (see above). In an eye-fixed coordinate frame, however, the movements of both eyes in all paradigms would be named "purely torsional."

RESULTS

Figures 3 and 4 show the data of a typical example (*subject AK*) during paradigms I (Figs. 3, I and 4, I) and III (Figs. 3, III and 4, III). In both figures, the panels depict in descending order: torsional turntable position multiplied by (−1) and the three components of eye movement (torsional, vertical, horizontal).

Figure 3 represents the torsional turntable position (*top panel*), and the torsional (r_x), vertical (r_y), and horizontal (r_z) components (*bottom 3 panels*) of eye position (rotation vectors) during vestibular stimulation (0.3 Hz, ±30°). Traces of the right (solid line) and the left (dashed line) eye are plotted. In Fig. 3, I, during fixation of the far head-fixed target in front of the right eye, the ocular response to the turntable oscillation is mainly torsional, i.e., aligned with the stimulus axis, and nearly in phase. There are frequent torsional quick phases in the opposite direction of the slow phases (=vestibular nystagmus). Clearly, the amplitudes of the torsional traces (r_x) of the two eyes are not exactly equal. Also there are small divergent movements of the vertical (r_y) positions traces.

In Fig. 3, III, the component with the largest modulation is again torsional (r_x), but now the divergent movement of the vertical traces (r_y) have increased (arrows) compared to the situation when the subject fixed upon the far head-fixed target in front of the right eye. The horizontal position (r_z) of the right eye is approximately zero, and the left eye points 12° to the right, as both eyes converge upon the near head-fixed target in front of the right eye. There was a small offset of 2–3° between the torsional traces of the right and left eye.

Figure 4 depicts the turntable movement and the deviation between the two eyes in the velocity domain. The angular velocity of ocular deviation $\Delta\omega$ was defined by the difference between the angular velocity vectors of the right and left eye

$$\Delta\omega = \omega(\text{right eye}) - \omega(\text{left eye})$$

Because angular velocity vectors represent the orientation of the instantaneous rotation axis of the eyes in the head, on which we focused our interest, the subsequent statistics were based on this description of the data. The amplitude of the torsional deviation velocity ($\Delta\omega_x$) was larger in paradigm I (Fig. 4, I) than in paradigm III (Fig. 4, III). The amplitude of the vertical deviation velocity ($\Delta\omega_y$), however, was smaller during fixation upon the far head-fixed target in front of the right eye (Fig. 4, I) than during convergence upon the near head-fixed target in front of the right eye (Fig. 4, III). The horizontal deviation velocity ($\Delta\omega_z$), as expected from the previous figures depicting position traces, did not modulate with the torsional vestibular stimulus.

To further process the data, the following sine function (s) with two harmonics was fitted to the torsional, vertical, and horizontal components of angular deviation velocity

$$s = A_{\Delta\omega} \cdot \sin(2\pi f \cdot t + \varphi) + B_{\Delta\omega} \cdot \sin(2 \cdot 2\pi f \cdot t + \varphi) + C_{\Delta\omega}$$

where $A_{\Delta\omega}$ and $B_{\Delta\omega}$ are the amplitudes of the first and second harmonic, respectively, f is the frequency, φ is the phase, and $C_{\Delta\omega}$ is the offset. The frequency (f), as determined by the chair signal, was kept constant, while $A_{\Delta\omega}$, $B_{\Delta\omega}$, $C_{\Delta\omega}$, and φ were iteratively optimized by a nonlinear least-square algorithm based on the Levenberg-Marquardt method (Matlab-function lsqnonlin.m). The subsequent analysis was based on the amplitude of the first harmonic ($A_{\Delta\omega}$). The amplitude of the second harmonic ($B_{\Delta\omega}$) was always less than 20% of the first harmonic.

Figure 5 summarizes the amplitudes of the angular deviation velocity ($A_{\Delta\omega}$) computed from the data of the same subject on which the three previous figures were based. The abscissa contains the three conditions of fixation (I: far head-fixed target in front of the right eye; II: far head-fixed target to the right; III: near head-fixed target in front of the right eye). Values for the binocular (○– – –○) and right-eye (●——●) viewing conditions show a similar pattern in all panels: the torsional deviation velocity [$A_{\Delta\omega(x)}$; *top panel*] did not change between paradigms I and II, but decreased in paradigm III. For the vertical deviation velocity [$A_{\Delta\omega(y)}$; *middle panel*], paradigms I and II again lead to similar values, while in paradigm III the velocity showed a striking increase. The values for the horizontal deviation velocity [$A_{\Delta\omega(z)}$; *bottom panel*] were roughly the same in all three paradigms.

To visualize to what extent the different components of the angular deviation velocity ($A_{\Delta\omega}$) were influenced by the convergence angle (α), we plotted these two parameters against each other in Fig. 6. In all three panels, the four data points at a convergence angle $\alpha = 0°$ stem from paradigms I and II (monocular: ●; binocular: ○). The data point at $\alpha = 6.5°$ convergence corresponds to the monocular viewing condition (III_R), and the data point at $\alpha = 11.5°$ to the binocular viewing condition (III) in paradigm III.[1] Clearly, only the vertical deviation velocity (*middle panel*) increased as a function of the convergence angle. Two lines (dashed and dotted) were added to the *middle panel* of the figure.

1) The dashed line (straight line) represents the prediction of vertical deviation velocity based on the following assumptions. *A*) The vertical deviation velocity is zero in the absence of convergence. *B*) Both eyes rotate such that the head-fixed target always stays on the fovea. *C*) The gain of ocular counterroll during convergence is the same as during viewing of the far target. In this subject, the average torsional vestibuloocular gain of both eyes during binocular viewing of the far target was $g_x = 0.56$. This corresponds to a torsional angular velocity of $A_{\omega_x} = 31.7°/s$ at a maximal chair velocity of 56.5°/s (0.3 Hz, ±30°). From these three assumptions, the first-order linear regression relating the convergence angle (α) and the average torsional velocity of both eyes [$A_{\omega(x)}$] with the angular deviation velocity [$A_{\Delta\omega(y)}$] is

$$A_{\Delta\omega(y)} = \tan(\alpha) \cdot A_{\omega(x)}$$

2) The dotted line (slightly broken line) is based on assumptions *A* and *B* but takes into account that the gain of ocular counterroll decreased with convergence. The measured dynamic counterroll gains at the convergence angles $\alpha = 6.5°$ and $\alpha = 11.5°$ were 0.38 and 0.36, respectively.

[1] The convergence angle α was smaller during monocular viewing than during binocular viewing in all but one subject (*OB*).

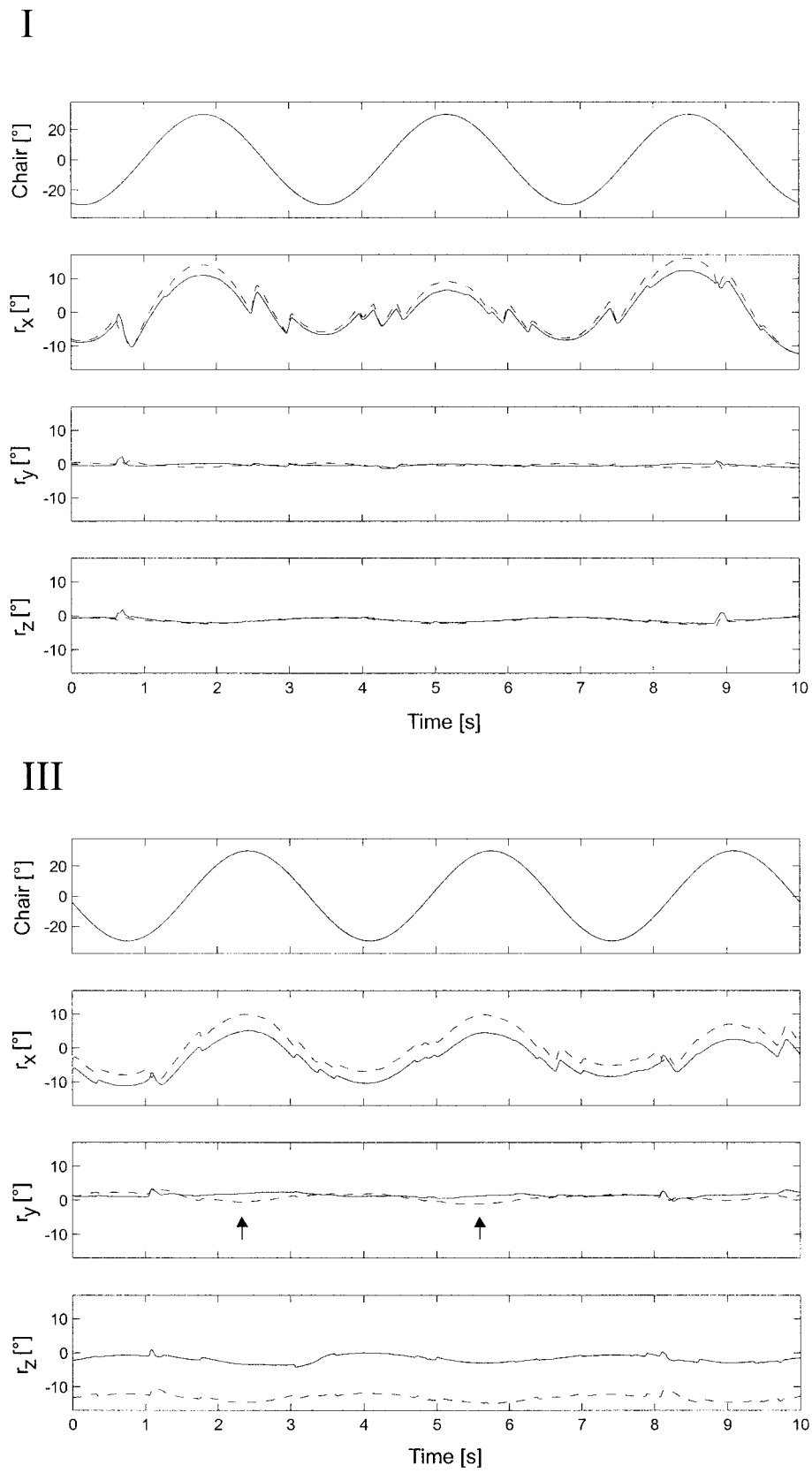

FIG. 3. Example of turntable and eye position during torsional vestibular stimulation with both eyes viewing in paradigms I and III (*subject AK*). *Top panels*: torsional position of the turntable (Chair). *Bottom 3 panels*: torsional (r_x), vertical (r_y), and horizontal (r_z) components of eye rotation vectors. Solid line, right eye; dashed line, left eye. Arrows: periods of vertical divergence. Anticompensatory quick phases are restricted to the torsional trace. Transient movements away from the baseline seen in the vertical and horizontal traces are due to blinks.

The data points in the *middle panel* of Fig. 6 are oriented more parallel to the theoretical regression, that takes into account the decrease of the torsional gain with convergence (dotted line), and less parallel to the regression that is based on a constant torsional gain. Thus the amount of vertical deviation velocity seems to depend on the torsional gain *and* the convergence angle. The offset of the data points at zero degree convergence probably represents the known small skew devi-

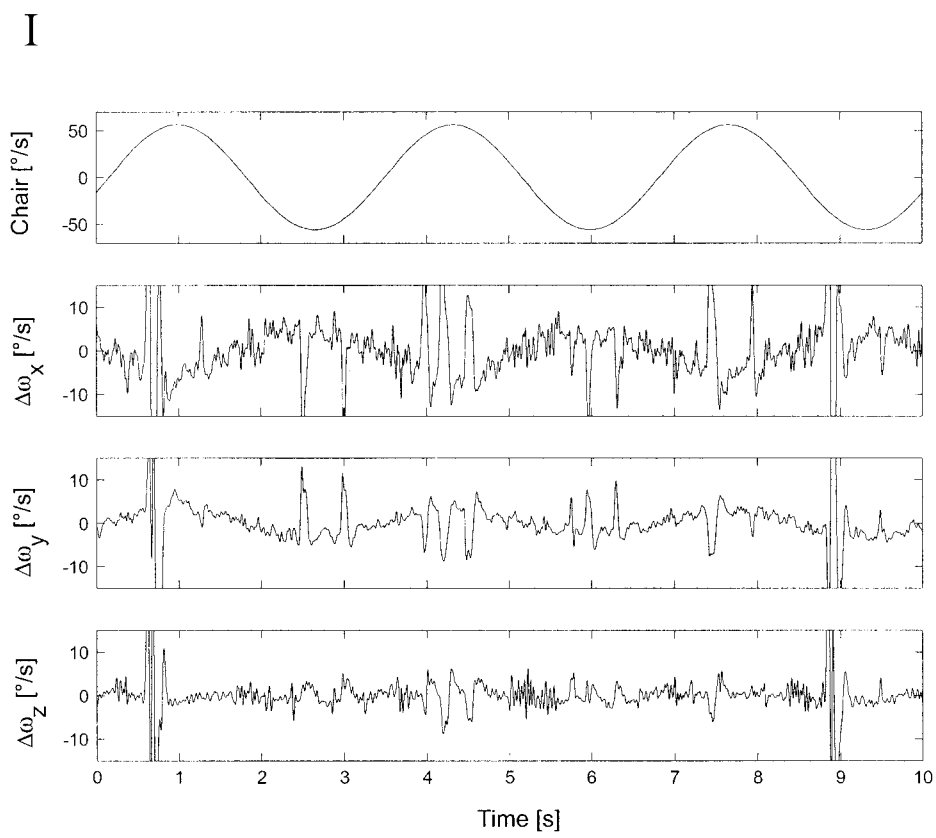

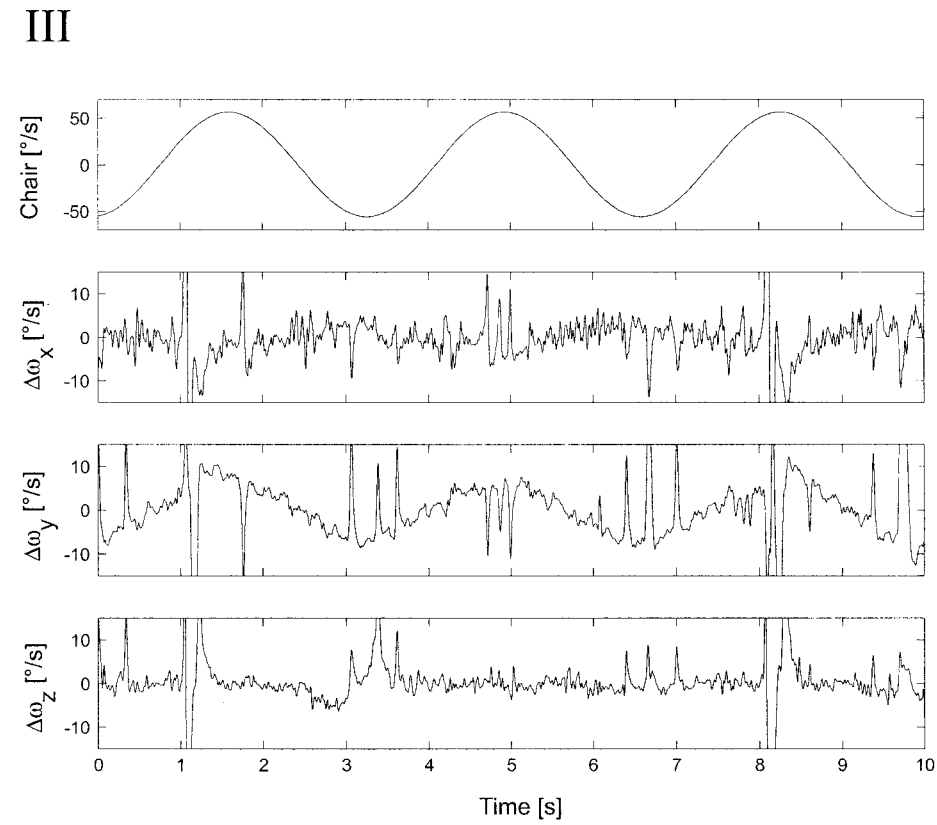

FIG. 4. Difference of angular velocity vectors between the right and left eye. Same data as in Fig. 3. Chair: torsional turntable velocity. $\Delta\omega_x$, torsional; $\Delta\omega_y$, vertical; $\Delta\omega_z$, horizontal components of eye deviation velocity (right eye minus left eye).

ation observed during torsional VOR of healthy human subjects (Jauregui-Renaud et al. 1998).

Figure 7 demonstrates the effect of the different paradigms on the gain of the torsional VOR in *subject CB* (Fig. 7, *A* and *B*) and in all six subjects measured (Fig. 7, *C* and *D*). The gains of the right (●) and the left (○) eyes are plotted separately. The *left panels* (Fig. 7, *A* and *C*) depict the gains during binocular, and the *right panels* (Fig. 7, *B* and *D*) the gains during mon-

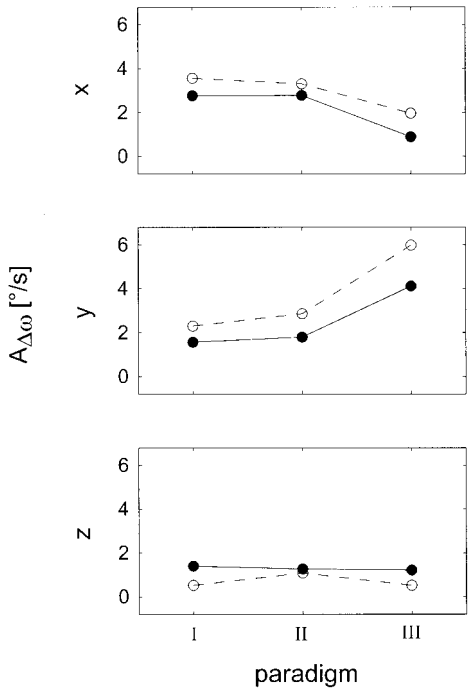

FIG. 5. Amplitudes of the 3-dimensional angular deviation velocity ($A_{\Delta\omega}$) in *subject AK* for the different paradigms (I, II, and III). ○– – –○, values during binocular fixation; ● —— ●, values during monocular fixation (left eye covered). *x*, torsional; *y*, vertical; *z*, horizontal components of $A_{\Delta\omega}$.

ocular fixation of the head-fixed target. On the *top panels* (Fig. 7, *A* and *B*) the lines connect the single data points; on the *bottom panels* (Fig. 7, *C* and *D*), the lines connect the medians.

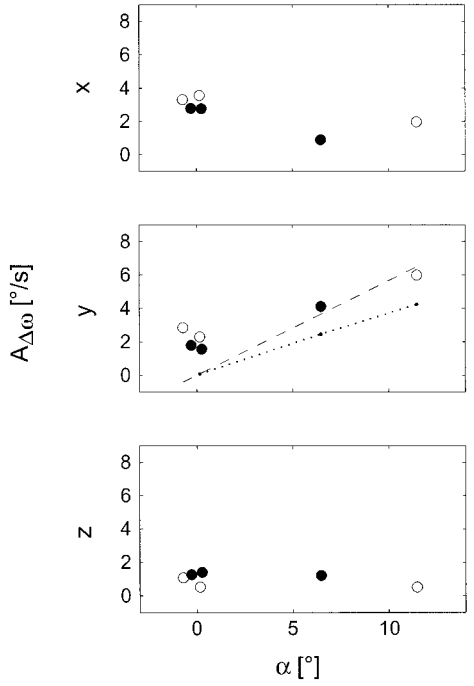

FIG. 6. Amplitudes of the 3-dimensional angular deviation velocity ($A_{\Delta\omega}$) as a function of the convergence angle (α). Same data as in Fig. 5 (*subject AK*). ○, values during binocular fixation; ●, values during monocular fixation (left eye covered). *x*, torsional; *y*, vertical; *z*, horizontal components of $A_{\Delta\omega}$. Dashed line (straight) represents the prediction of vertical deviation velocity if the gain of ocular counterroll is independent of the target position. Dotted line (slightly broken) takes into account the decreased gain of ocular counterroll with convergence.

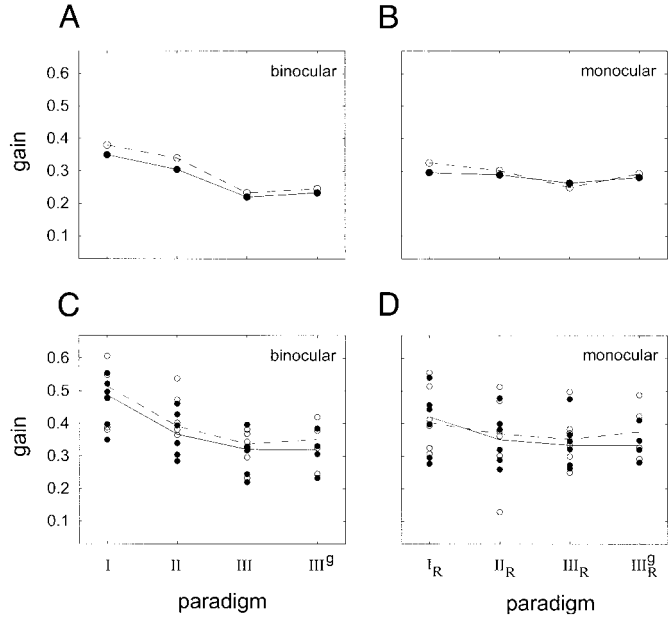

FIG. 7. Gain of the torsional vestibuloocular reflex in the different paradigms during binocular (*left panels*) or monocular (*right panels*) fixation. ● —— ●, gain values of the right eyes; ○– – –○, gain values of the left eyes. I, II, III, and III^g: paradigms during binocular fixation. I_R, II_R, III_R, and III^g_R: paradigms during monocular fixation (left eye covered). *A* and *B*: *subject CB* (lines connect values). *C* and *D*: all 6 subjects (lines connect median values).

The gains of both eyes were very similar. In both the binocular and monocular viewing conditions, fixation of the far head-fixed target in front of the right eye (I, I_R) during torsional VOR resulted in the highest gains. Note, however, that the gains during binocular straight-ahead far viewing (Fig. 7*C*, I; median gains right eye: 0.49; left eye: 0.51) were considerably higher than during monocular straight-ahead far viewing (Fig. 7*D*, I_R; right eye: 0.42; left eye: 0.40). These gain differences were significant in the paired *t*-test ($P < 0.001$).

Already fixing with both eyes upon the far head-fixed target 13.5° to the right led to a decrease of the gain during both binocular (Fig. 7*C*, II; right eye: 24.6%; left eye: 23.8%) and monocular viewing (Fig. 7*D*, II_R; right eye: 16.6%; left eye: 8.5%). These numbers were much higher than one would have expected if the gain vector had only changed its orientation by 13.5° to the right, but not its length; in this case the torsional gain would have only decreased by $1 - \cos(13.5°) = 2.8\%$. During convergence on the near head-fixed target in front of the right eye, we measured an additional decrease of the gain; the gain reduction compared to fixation of the far head-fixed target in front of the right eye (100%) was more prominent in the binocular (Fig. 7*C*, III; right eye: 34.2%; left eye: 34.4%) than in the monocular (Fig. 7*D*, III_R; right eye: 20.7%; left eye: 12.5%) viewing condition. There was no further decrease of torsional gains when the subjects wore the glasses with +3 dpt (Fig. 7, *C* and *D*, III^g and III^g_R), i.e., accommodation was not a relevant factor in the reduction of the torsional VOR gain during convergence.

So far we have shown that the different paradigms influenced both the vertical deviation velocity and the gain of the torsional VOR. We asked whether there was a linear correlation between the convergence angle (independent variable) and the vertical deviation velocity (dependent variable). To explore this question, we pooled the data of all six subjects collected during the four different paradigms into two datasets: one from

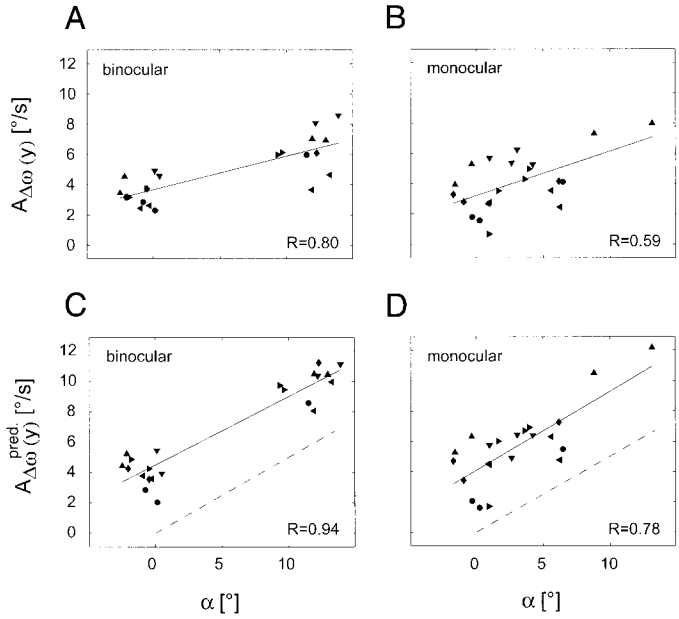

FIG. 8. Vertical amplitude of angular deviation velocity as a function of the convergence angle (α). In each subject ($n = 6$; different symbol for every individual) values from all tested paradigms are pooled. Data from paradigms with binocular (*left panels*) and monocular (*right panels*) viewing are given separately. Solid lines: computed linear regressions; *R*-values were highly significant ($P < 0.01$) in all panels. Dashed lines: predicted line with a slope of 0.5 and no offset. $A_{\Delta\omega(y)}$: measured vertical deviation velocity (*A* and *B*). $A^{pred.}_{\Delta\omega(y)}$: predicted vertical deviation velocity, when the data are normalized to an ocular counterroll gain of 0.5 in all subjects and paradigms (*C* and *D*).

the binocular (I, II, III, III^g) and the other from the monocular (I_R, II_R, III_R, III^g_R) viewing conditions. The *top panels* on Fig. 8 present these two scatter plots. In both conditions we found highly significant ($P < 0.01$) correlations between the convergence angle (α) and vertical deviation velocity [$A_{\Delta\omega(y)}$]. The correlation for the binocular viewing conditions (Fig. 8*A*) was superior compared to the monocular viewing conditions (Fig. 8*B*). In part, this was due to the fact that during monocular fixation upon the near head-fixed target convergence angles typically did not reach values above 10°.

The hypothesis that led to these experiments was that, at a specific convergence angle, an increase in counterroll gain should directly lead to an increase of the vertical deviation velocity if the head-fixed target is kept on the foveae of both eyes. But since the gain of ocular counterroll was different between subjects and also decreased with convergence, the direct relation between the convergence angle and the vertical deviation velocity could better be shown by normalizing the data to a constant gain of ocular counterroll. In line with our hypothesis, the predicted vertical deviation velocity [$A^{pred.}_{\Delta\omega(y)}$] at a fixed counterroll gain of 0.5 was computed from the measured vertical deviation velocity [$A_{\Delta\omega(y)}$] and the measured counterroll gain (g_x) by

$$A^{pred.}_{\Delta\omega(y)} = A_{\Delta\omega(y)} \cdot \frac{0.5}{g_x}$$

The two *bottom panels* in Fig. 8 depict this relation during the binocular (Fig. 8*C*) and monocular (Fig. 8*D*) viewing conditions in all six subjects. If the convergence angle (α) and the torsional gain (g_x) in combination are the only predictors of the vertical deviation velocity [$A_{\Delta\omega(y)}$] and the torsional gain is normalized to 0.5 [leading to $A^{pred.}_{\Delta\omega(y)}$], the data points should lie on the dashed line that goes through zero and has a slope of 0.5. The slopes of the linear regressions in both conditions were indeed close to 0.5 (binocular viewing conditions: 0.45; monocular viewing condition: 0.52), but there was an offset around 4°/s in both conditions, which corresponds to the physiological skew deviation observed during torsional VOR (Betts et al. 1995; Jauregui-Renaud et al. 1998; Kori et al. 2001). This small vertical deviation velocity had no visual consequences, since, during the binocular viewing conditions, none of the subjects reported any diplopia. The fact that the normalization of the torsional gain also led to an increase of the correlation coefficients indicates that indeed the individual values of the counterroll gain influenced the vertical deviation velocities of the eyes.

DISCUSSION

This study in healthy human subjects demonstrates that convergence upon a near head-fixed target during torsional head oscillation about the nasooccipital axis leads to ocular movements that are different in the two eyes. The convergence-induced reorientation of the ocular rotation axes during the torsional VOR ensures that the lines-of-sight of both eyes remain directed onto the visual target, i.e., the axes about which the two eyes rotate during the torsional vestibular stimulation are parallel to the respective lines-of-sight. As a consequence, the vertical velocity (expressed in head-fixed coordinates) differs between the two eyes. This vertical deviation velocity depends on the gain of the dynamic ocular counterroll and the convergence angle, but not on accommodation. In addition, by lowering the gain of the torsional VOR during convergence, the CNS reduces the vertical deviation velocity needed for directing both lines-of-sight to the visual target.

So far, little was known about the kinematical changes of eye movements induced in the context of visual VOR cancellation. Most investigations on how the CNS suppresses ocular responses during vestibular stimulation were focused on the dynamical aspects of the relation between vestibular input and ocular motor output (Barnes et al. 1978; Gauthier and Vercher 1990; Robinson 1982). When the technology to measure eye movements about all principal axes of rotation (horizontal, vertical, torsional) was established, it became possible to study the effect of visual suppression on the orientation of the ocular rotation axes (Collewijn et al. 1985; Robinson 1963). The first series of experiments concentrated on whether the torsional VOR could be suppressed by vision, even though the pursuit system operates only in two dimensions (horizontal and vertical). In rhesus monkeys, postrotatory torsional nystagmus could not be cancelled during the first few seconds, i.e., there was only a late suppressive effect, which was attributed to the optokinetic system (Straumann et al. 1992). In humans who actively oscillated their heads at about 0.5 Hz, the gain of the torsional VOR dropped from 0.61 in the dark to 0.46 when subjects were viewing a visual display (Leigh et al. 1989). Thus despite the fact that the pursuit system is not sensitive for rotations about the line-of-sight and despite the very low torsional optokinetic gain in upright position (Collewijn et al. 1985), visual suppression was able to reduce the torsional VOR gain by 25%.

The next step was to elicit the VOR in all directions (horizontal, vertical, torsional) and, at the same time, to present fixation targets at different horizontal and vertical positions.

Misslisch et al. found that the angular velocity vectors of the eyes were always aligned with the line-of-sight (Misslisch et al. 1996). Thus the pursuit system cancelled the horizontal and vertical components of *retinal velocity*. In addition, the remaining *angular velocity vector*, which was oriented parallel to the ocular rotation axis, was decreased in length. This again suggested the existence of a second mechanism of VOR cancellation in addition to the mechanism by the pursuit system.

In the present experiments, which were restricted to visual suppression of the torsional VOR, we demonstrated that the same principles that apply to the fixation of far targets could be extended to convergence. We chose to study the effect of visual fixation during the VOR in the *torsional direction*, because, in this paradigm, it was easiest to demonstrate the effect of the direction of the line-of-sight on the kinematics of eye rotation. The angular velocity vectors of the two eyes were parallel with their lines-of-sight, and thus the rotation axes of the two eyes formed an angle that was close to equal to the convergence angle.

The results of our study demonstrate that, under the described conditions, the ocular system is successful in directing the rotation axes of the two eyes toward the fixation target during ongoing vestibular stimulation, even in the absence of visual feedback. This result agrees well with the reported high precision of binocular vertical alignment of fixations and saccades during convergence in tertiary positions (Collewijn 1994; Schor et al. 1994; Ygge and Zee 1995). The gain reduction of the torsional VOR induced by convergence, a phenomenon that has already been reported by earlier studies (Averbuch-Heller et al. 1997), facilitates the vertical alignment during fixation of a near target in the presence of a vestibular roll stimulation.

Can our findings be explained by the action of the smooth pursuit system during VOR cancellation? The following speaks against this hypothesis: for each eye, one would have to postulate a separate pursuit system, both for the afferent (detection of retinal velocity) and efferent (eye movement) pathways. To our knowledge there are no experimental findings that would support this assumption. Moreover, the fact that covering one eye does not lead to a change of its rotation axis also speaks against a significant role of the smooth pursuit system in VOR cancellation during convergence. It is more likely that the ocular motor system explicitly computes the correct 3D kinematics from the relevant parameters, i.e., the horizontal-vertical direction and depth of the target, and the gain of the torsional VOR at a given frequency. Such an algorithm of VOR cancellation is certainly able to stabilize the lines-of-sight of the two eyes on the target but also allows for a certain amount of torsional retinal slip that is equal in the two eyes. If such a mechanism is implemented, the question arises whether the impact of the pursuit system on VOR cancellation is rather weak. In fact, there are experimental findings that support a non-pursuit suppression mechanism of VOR cancellation; rarely one finds patients with disordered smooth pursuit, but intact VOR cancellation (Chambers and Gresty 1983). Similarly, some patients with deficient smooth pursuit eye movements can still smoothly track a moving target when both eye and head are moving (Grant et al. 1992). Probably the segregation of smooth pursuit and VOR cancellation is already implemented at the level of the cerebellum: in patients with spinocerebellar ataxia type 6, horizontal smooth pursuit was impaired, but the cancellation of the horizontal VOR was not affected (Takeichi et al. 2000). These behavioral data agree with lesional studies in squirrel monkeys: muscimol microinjections into the floccular region impaired ocular pursuit, but had little effect on VOR cancellation (Belton and McCrea 1999). Our finding that the torsional VOR gain during cancellation was reduced and even further decreased during convergence also indicates that other mechanisms than the pursuit system are involved in the visual cancellation of the VOR. How exactly the kinematical changes of the torsional VOR induced by convergence is implemented remains unclear. Possibly, active muscle pulleys play an important role in reorienting the ocular rotation axes during convergence (Demer et al. 2000).

The roll stimulus we applied in our experiments was not purely angular but also included a vertical linear component, because the rotation about the nasooccipital axis through the center of the head caused the labyrinths to be vertically translated in opposite directions (Seidman et al. 1995). Therefore it is possible that the vertical movement of the left eye, that points its line-of-sight toward the target in front of the right eye, is enhanced by the linear VOR. Future experiments must try to quantify the contribution of the linear VOR during torsional vestibular stimulation by applying head roll in total darkness about different axes through the head and varying convergence angles with (earth-horizontal axis) and without (earth-vertical axis) otolith activation.

In conclusion, ocular convergence on a head-fixed target during the VOR requires a substantial modification of binocular kinematics to prevent double vision. We have demonstrated this phenomenon for a frequency of 0.3 Hz, which is well below the natural frequencies of the head (Grossman et al. 1988). Thus it will be necessary to do the same analysis on the convergence-induced reorientation of ocular rotation axes at higher frequencies.

We thank A. A. Kori for valuable comments and help in part of the experiments, and A. Züger for technical support.

This work was supported by the Swiss National Science Foundation (3231-051938.97/3200-052187.97), the Betty and David Koetser Foundation for Brain Research, and the Freiwillige Akademische Gesellschaft, Basel.

REFERENCES

AVERBUCH-HELLER L, ROTTACH KG, ZIVOTOFSKY AZ, SUAREZ JI, PETTEE AD, REMLER BF, AND LEIGH RJ. Torsional eye movements in patients with skew deviation and spasmodic torticollis: responses to static and dynamic head roll. *Neurology* 48: 506–514, 1997.

BARNES GR, BENSON AJ, AND PRIOR AR. Visual-vestibular interaction in the control of eye movement. *Aviat Space Environ Med* 49: 557–564, 1978.

BELTON T AND MCCREA RA. Contribution of the cerebellar flocculus to gaze control during active head movements. *J Neurophysiol* 81: 3105–3109, 1999.

BETTS GA, CURTHOYS IS, AND TODD MJ. The effect of roll-tilt on ocular skew deviation. *Acta Otolaryngol Suppl* 520: 304–306, 1995.

CHAMBERS BR AND GRESTY MA. The relationship between disordered pursuit and vestibulo-ocular reflex suppression. *J Neurol Neurosurg Psychiatry* 46: 61–66, 1983.

COLLEWIJN H. Vertical conjugacy: what coordinate system is appropriate? In: *Contemporary Ocular Motor and Vestibular Research: A Tribute to David A. Robinson*, edited by Fuchs AF, Brandt T, Büttner U, and Zee DS. Stuttgart, Germany: Thieme, 1994, p. 296–303.

COLLEWIJN H, VAN DER STEEN J, FERMAN L, AND JANSEN TC. Human ocular counterroll: assessment of static and dynamic properties from electromagnetic scleral coil recordings. *Exp Brain Res* 59: 185–196, 1985.

DEMER JL, OH SY, AND POUKENS V. Evidence for active control of rectus extraocular muscle pulleys. *Invest Ophthalmol Vis Sci* 41: 1280–1290, 2000.

GAUTHIER GM AND VERCHER JL. Visual vestibular interaction: vestibulo-ocular reflex suppression with head-fixed target fixation. *Exp Brain Res* 81: 150–160, 1990.

GRANT MP, LEIGH RJ, SEIDMAN SH, RILEY DE, AND HANNA JP. Comparison of predictable smooth ocular and combined eye-head tracking behaviour in patients with lesions affecting the brainstem and cerebellum. *Brain* 115: 1323–1342, 1992.

GROSSMAN GE, LEIGH RJ, ABEL LA, LANSKA DJ, AND THURSTON SE. Frequency and velocity of rotational head perturbations during locomotion. *Exp Brain Res* 70: 470–476, 1988.

HEPP K. On Listing's law. *Commun Math Physics* 132: 285–292, 1990.

JAUREGUI-RENAUD K, FALDON M, CLARKE AH, BRONSTEIN AM, AND GRESTY MA. Otolith and semicircular canal contributions to the human binocular response to roll oscillation. *Acta Otolaryngol* 118: 170–176, 1998.

KORI AA, SCHMID-PRISCOVEANU A, AND STRAUMANN D. Vertical divergence and counterroll eye movements evoked by whole body position steps about the roll axis of the head in humans. *J Neurophysiol* 85: 671–678, 2001.

LEIGH RJ, MAAS EF, GROSSMAN GE, AND ROBINSON DA. Visual cancellation of the torsional vestibulo-ocular reflex in humans. *Exp Brain Res* 75: 221–226, 1989.

MISSLISCH H, TWEED D, FETTER M, DICHGANS J, AND VILIS T. Interaction of smooth pursuit and the vestibuloocular reflex in three dimensions. *J Neurophysiol* 75: 2520–2532, 1996.

MISSLISCH H, TWEED D, FETTER M, SIEVERING D, AND KOENIG E. Rotational kinematics of the human vestibuloocular reflex. III. Listing's law. *J Neurophysiol* 72: 2490–2502, 1994.

ROBINSON DA. A method of measuring eye movement using a scleral search coil in a magnetic field. *IEEE Trans Biomed Eng* 10: 137–145, 1963.

ROBINSON DA. A model of cancellation of the vestibulo-ocular reflex. In: *Functional Basis of Ocular Motility Disorders*, edited by Lennerstrand G, Zee DS, and Keller EL. New York: Pergamon, 1982, p. 5–13.

SCHOR CM, MAXWELL JS, AND STEVENSON SB. Isovergence surfaces: the conjugacy of vertical eye movements in tertiary positions of gaze. *Ophthalmic Physiol Opt* 14: 279–286, 1994.

SEIDMAN SH, TELFORD L, AND PAIGE GD. Vertical, horizontal, and torsional eye movement responses to head roll in the squirrel monkey. *Exp Brain Res* 104: 218–226, 1995.

STRAUMANN D, SUZUKI M, HENN V, HESS BJ, AND HASLWANTER T. Visual suppression of torsional vestibular nystagmus in rhesus monkeys. *Vision Res* 32: 1067–1074, 1992.

STRAUMANN D, ZEE DS, SOLOMON D, LASKER AG, AND ROBERTS D. Transient torsion during and after saccades. *Vision Res* 35: 3321–3334, 1995.

TAKEICHI N, FUKUSHIMA K, SASAKI H, YABE I, TASHIRO K, AND INUYAMA Y. Dissociation of smooth pursuit and vestibulo-ocular reflex cancellation in SCA-6. *Neurology* 54: 860–866, 2000.

YGGE J AND ZEE DS. Control of vertical eye alignment in three-dimensional space. *Vision Res* 35: 3169–3181, 1995.

ZEE DS. Suppression of vestibular nystagmus. *Ann Neurol* 1: 207, 1977.